



Molecular Crystals and Liquid Crystals Incorporating Nonlinear Optics

Publication details, including instructions for authors and
subscription information:

<http://www.tandfonline.com/loi/gmcl17>

Guest-Host Polymers for Nonlinear Optics

K. D. Singer^a, W. R. Holland^a, M. G. Kuzyk^a, G. L. Wolk^c & P.
A. Cahill^b

^a AT&T Bell Laboratories, P.O. Box 900, Princeton, NJ, 08540

^b Sandia National Laboratories, Division 1811, Albuquerque, NM,
87185-5800

^c Department of Physics, Washington State University, Pullman,
WA, 99164-2814

Version of record first published: 22 Sep 2006.

To cite this article: K. D. Singer, W. R. Holland, M. G. Kuzyk, G. L. Wolk & P. A. Cahill (1990):
Guest-Host Polymers for Nonlinear Optics, *Molecular Crystals and Liquid Crystals Incorporating
Nonlinear Optics*, 189:1, 123-136

To link to this article: <http://dx.doi.org/10.1080/00268949008037227>

PLEASE SCROLL DOWN FOR ARTICLE

Full terms and conditions of use: <http://www.tandfonline.com/page/terms-and-conditions>

This article may be used for research, teaching, and private study purposes. Any
substantial or systematic reproduction, redistribution, reselling, loan, sub-licensing,
systematic supply, or distribution in any form to anyone is expressly forbidden.

The publisher does not give any warranty express or implied or make any
representation that the contents will be complete or accurate or up to date. The
accuracy of any instructions, formulae, and drug doses should be independently
verified with primary sources. The publisher shall not be liable for any loss, actions,
claims, proceedings, demand, or costs or damages whatsoever or howsoever caused
arising directly or indirectly in connection with or arising out of the use of this material.

Guest-Host Polymers for Nonlinear Optics

K. D. SINGER, W. R. HOLLAND, M. G. KUZYSK,† and G. L. WOLK

AT&T Bell Laboratories. P.O. Box 900, Princeton, NJ 08540

and

P. A. CAHILL

Sandia National Laboratories, Division 1811, Albuquerque, NM 87185-5800

Much recent interest in second-order nonlinear optical materials and devices has focussed on poled polymer films, which derives mainly from their large nonlinear optical coefficients, ease of fabrication, and high optical quality. Progress has been rapid in producing stable, efficient materials, and in building demonstration devices. The second-order nonlinear optical properties arise from the orientational order induced in a collection of highly nonlinear molecules incorporated in a glassy polymer matrix. In this paper, the physics of alignment is presented, as well as progress in the development of new polymeric materials. Electro-optic devices have been fabricated and tested confirming the promise of polymeric nonlinear optical materials. An approach to phase-matched second harmonic generation which is highly compatible with molecular-polymer materials based on anomalous dispersion in nonlinear optical molecules is also presented.

I. POLED POLYMER FILMS

Until recently, most research into organic second-order nonlinear optical materials was limited to crystalline materials since the requirements for a noncentrosymmetric bulk phase could be met with molecular and polymeric crystals that happen to condense in a noncentrosymmetric point group.¹ However, for guided-wave applications, a thin film technology would be more desirable. To achieve this, systems consisting of the nonlinear optical molecules incorporated into polymer glasses, liquid crystals, and liquid crystal polymers have been investigated.² The difficulties in processing that are required to obtain optical quality materials are reduced. For second-order nonlinearities, an alignment process, such as electric field poling, is required to break the center of symmetry inherent in these materials. However, the reduction in number density and alignment attainable with realistic poling fields requires molecules with exceptionally large nonlinear optical susceptibilities in order to obtain bulk materials with nonlinear coefficients large enough to produce useful devices.

†Present address: Department of Physics, Washington State University, Pullman, WA 99164-2814.

1.1 Nonlinear Optics In Films

As in molecular crystalline materials, the origin of the optical nonlinearities in guest-host polymer materials arises from the incorporated nonlinear optical moieties. However, the position and orientation of the moieties in the polymer host is not measurable as in crystalline materials, and so the relationship between the molecular and bulk susceptibility must be deduced from the thermodynamic potentials responsible for molecular motion during the poling and processing of the material. These potentials can arise from internal forces such as those responsible for liquid crystalline order, or external forces, such as those due to the poling field. Optical harmonic generation can be used to probe the molecular orientational distributions that result from these forces. The knowledge of these distributions, and the factors contributing to them are crucial since they determine the tensor components of the nonlinear susceptibility.^{3,4}

In organic molecular systems, such as molecular crystals and guest-host-polymer structures, the nonlinear optical moieties usually behave according to an oriented gas model. These interactions are dominated by dipolar, or van der Waals forces, so that the macroscopic polarization, $P_i(t)$, is calculated by evaluating the thermodynamic average of the electronic contributions of the individual molecules, $p_i(t)$ (ignoring nonlocal effects):

$$P_i(t) = N \langle p_i(t) \rangle_i \quad (1)$$

where N is the molecular number density. In general, the molecules whose polarizations are summed using Equation (1) exist within a thermal environment, so that the summation is expressed as a thermodynamic average, which, for an n th order nonlinear optical process is given by,

$$\chi_{ijkl\dots}^{(n)} = N \langle \xi_{IJKL\dots}^* \rangle_{ijkl\dots}, \quad (2)$$

where $\langle \xi_{IJKL\dots}^* \rangle_{ijkl\dots}$ is the $ijkl\dots$ th component of the orientational average of the molecular n th order susceptibility, and where the $*$ denotes that the local field effects have been included with the susceptibility. The indices I, J, K, L, \dots span x, y, z denote the molecular frame, and i, j, k, l, \dots span $1, 2, 3$ the laboratory frame. The orientational ensemble average for a tensor $\xi_{IJKL\dots}$ is calculated using the following integral:

$$\langle \xi_{IJKL\dots} \rangle_{ijkl} = \int_0^{2\pi} d\theta \int_0^\pi \sin\theta d\theta \int_0^{2\pi} d\psi \xi_{IJKL\dots} a_{iI} a_{jJ} a_{kK} a_{lL} \dots G(\phi, \theta, \psi), \quad (3)$$

where $G(\phi, \theta, \psi)$ is the normalized orientational distribution function and the a_{uU} rotation matrices, both of which are functions of the Euler angles ϕ , θ , and ψ . The bulk nonlinear response of an organic medium, then, is determined by the local field corrected molecular hyperpolarizabilities, the density of molecular units, and the orientational distribution of the molecules. It should be noted here that the use of a thermodynamic ensemble average implies that each particle experiences

a mean field potential. However, if short range interactions are strong enough to cause aggregation, then consideration of these interactions is required in the ensemble averages.

For noncrystalline materials, the orientational distribution function determines the nonlinear optical properties, and depends on the details of the interactions between molecules which are generally not known. The form of the orientational distribution function used in averaging over the molecular ensemble reflects the macroscopic symmetry of the medium. For a uniaxial phase with its symmetry axis parallel to the z-axis, the orientational distribution function $G(\phi, \theta, \psi)$ is independent of ϕ , and can be expanded in terms of spherical harmonics. Many nonlinear optical moieties have a large component of β along the ground state dipole moment, resulting in uniaxial symmetry where $G(\theta, \psi)$ is independent of ψ . $G(\theta)$ can then be expanded in terms of Legendre polynomials $P_l(\cos\theta)$,

$$G(\theta) = \sum_{l=0}^{\infty} \frac{(2l+1)}{2} A_l P_l(\cos\theta), \quad (4)$$

with the coefficients A_l determined from Equation (4) as,

$$\langle P_l \rangle \equiv A_l = \int_0^{\pi} \sin\theta d\theta G(\theta) P_l(\cos\theta). \quad (5)$$

The A_l are ensemble averages of the P_l and are defined as microscopic order parameters. For systems whose order is characterized solely by θ , the distribution of molecules is represented by the summation over successively higher orders of P_l . The odd-ordered polynomials P_l give the "polar" order. If molecular dipoles are arranged centrosymmetrically so that the net moment is zero, these terms are all zero. The even P_l give the angular distribution of molecules without distinguishing dipolar direction. General expressions for the even and odd order nonlinear susceptibilities are written in terms of $P(\theta)$ for axially symmetric molecules in an optically uniaxial medium,

$$\begin{aligned} \chi_{ijk\dots}^{(2n)} &= \sum_{m=0}^n u_{ijk\dots}^{(2m+1)} \langle P_{2m+1} \rangle, \\ \chi_{ijkl\dots}^{(2n+1)} &= \sum_{m=0}^{n+1} u_{ijkl\dots}^{(2m)} \langle P_{2m} \rangle. \end{aligned} \quad (6)$$

In these expressions, $u_{lmn\dots}^{(k)} = N\xi_{lmn\dots}^{(k)}$ where $\xi_{lmn\dots}^{(k)}$ are linear combinations of local field-corrected molecular hyperpolarizabilities and N the number density. The n th rank tensor yields a limited number of distribution moments, and for a medium with zero odd-order $\langle P_l \rangle$, even-order χ are zero. For a one dimensional molecule,

Equations (6) reduce to,⁵

$$\chi_{333}^{(2)} = N\beta_{zzz}^* \left[\frac{3}{5} \langle P_1 \rangle + \frac{2}{5} \langle P_3 \rangle \right] \quad (7)$$

and

$$\chi_{113}^{(2)} = \chi_{131}^{(2)} = \chi_{311}^{(2)} = N\beta_{zzz}^* \left[\frac{1}{5} \langle P_1 \rangle - \frac{1}{5} \langle P_3 \rangle \right] \quad (8)$$

where β_{zzz}^* is the local field corrected hyperpolarizability.

If known forces are acting on the molecular ensemble, the nonlinear optical susceptibility can be determined from the thermodynamic potentials acting on the ensemble. For a Gibbs distribution,

$$G(\theta) = \frac{\exp[-U/kT]}{\int_{-1}^{+1} d(\cos\theta) \exp[-U/kT]}. \quad (9)$$

The U is the mean-field potential describing the internal and external forces acting on the ensemble. This can be applied to electric field poling in molecular-polymeric materials. The poling process begins by placing the polymer with incorporated nonlinear optical molecules in an electric field while the polymer is in a state where the molecules are free to rotate. For thermoplastic materials, this is accomplished by raising the temperature above the glass transition temperature, and for thermoset materials, the poling is carried out in the uncured state. With the field applied, the polymer is then either cooled to room temperature following anneal for thermoplastics or cure for thermosets. The potential in the liquid-like poling state is given by,

$$U = -m^* E_p P_1(\cos\theta) \quad (10)$$

where m^* is the local field dressed ground state dipole moment, and E_p is the poling field. If a material possesses axial order as described by $\langle P_2 \rangle$ and $\langle P_4 \rangle$, electric field poling results in³

$$\chi_{333}^{(2)} = N\beta_{zzz}^* \frac{m_z^* E_p}{kT} \left[\frac{1}{5} + \frac{4}{7} \langle P_2 \rangle + \frac{8}{35} \langle P_4 \rangle \right], \quad (11)$$

and

$$\chi_{113}^{(2)} = \chi_{131}^{(2)} = \chi_{311}^{(2)} = N\beta_{zzz}^* \frac{m_z^* E_p}{kT} \left[\frac{1}{15} + \frac{1}{21} \langle P_2 \rangle - \frac{4}{35} \langle P_4 \rangle \right]. \quad (12)$$

The effect of other orienting forces, either internal as in liquid crystals or external,

as described below, will contribute to the susceptibility through the parameters $\langle P_2 \rangle$ and $\langle P_4 \rangle$. These are parameters that exist independent of the poling field. If the poling field is strong enough, these parameters will change through an interaction quadratic in the dipolar orienting energy.

1.2 Poling under Uniaxial Stress

We can further develop this formalism by considering the effect of electric field poling of a material under uniaxial stress.⁶ The potential, in this case, is given by

$$U = -m^* E_p P_1(\cos\theta) + b P_2(\cos\theta) \quad (13)$$

where the first term describes an electric poling field, and the second term describes the stress potential. Second harmonic generation can then be used to study the molecular flow under stress of the doped polymer, or, conversely, the stress can be used to control the nonlinear optical properties of the polymer.

In order to examine the effect of compressive stress applied perpendicular to the plane of a polymer film, the formalism leading to Equation (6) is applied in three steps.⁷ First, the susceptibility is calculated assuming an undetermined potential leading to Equations (7)–(8). Then Equations (11)–(12) can be applied. Finally, the effect of stress is added.

The first four order parameters can be determined from the form of the nonlinear optical tensor. A dipole experiences a polar force in the presence of an electric field and results in a nonzero $\langle P_1 \rangle$ in contrast to the effects of stress described in terms of the potential b , which results in a nonzero value of $\langle P_3 \rangle$ in the presence of the field.⁷ The ratio $\alpha = \langle P_3 \rangle / \langle P_1 \rangle$ can be shown to be a function of the stress and can be used to determine the orientational order of the molecules.⁷

Second harmonic generation is used to determine the ratio of the order parameters, α . The angular dependence of the second harmonic is measured as a function of incident angle for both s - and p -polarized fundamental and p -polarized second harmonic.⁸ The ratio of the second harmonic power for the two input polarizations can be used to determine a , the tensor ratio of the second order susceptibility. The doped films are made by spin coating on Indium Tin Oxide (ITO) coated substrates, and pressing two such coated substrates into a sandwich above the glass transition temperature. The poling field is applied with the ITO electrodes when above the transition temperature and removed after reaching room temperature. Table I shows the properties of the two measured films, and Figure 1 shows the dependence of orientational distribution function on the stress for a fixed poling field. The molecular flow outward from the stress axis is apparent.

1.3 New Materials

Enhanced second order nonlinear optical properties have been attained by corona poling thin films of a highly efficient dicyanovinyl azo dye molecule which was incorporated as a side chain on a methacrylate polymer.⁹ Second harmonic generation was measured for a thin corona-poled film of a dicyanovinyl azo dye incorporated in the side-chain methacrylate polymer shown in Figure 2. Measure-

TABLE I
Film parameters for PMMA doped with Disperse Red 1 dye

Film #	Dye Number Density N ($10^{20}/\text{cm}^3$)	Thickness (μm)	Poling Field E_p (MV/cm)	Stress $T_s(\text{dyne}/\text{cm}^2) \times 10^7$	a
1	2.42	4.0	0.60	0.00	0.33
2	1.08	4.9	0.25	3.71	0.7

ments were performed at a wavelength of $1.58\text{ }\mu\text{m}$ as a function of incident angle for both p - and s -polarized incident light. From these measurements the form and magnitude of the second harmonic coefficient tensor were determined, as shown in Table II.

The magnitudes of the second harmonic coefficients in Table II are considerably larger than films previously reported.³ This increase is due to the incorporation of a new nonlinear optical dye¹⁰ and the introduction of corona poling. In addition, the side-chain polymer optical nonlinearity due to poling was found to be considerably more stable than films with molecules dissolved in a polymer matrix.

2. DEVICES

The geometry of poled polymer films is amenable to the formation of guided-wave electro-optic and nonlinear optical devices. The requirements of electro-optic and

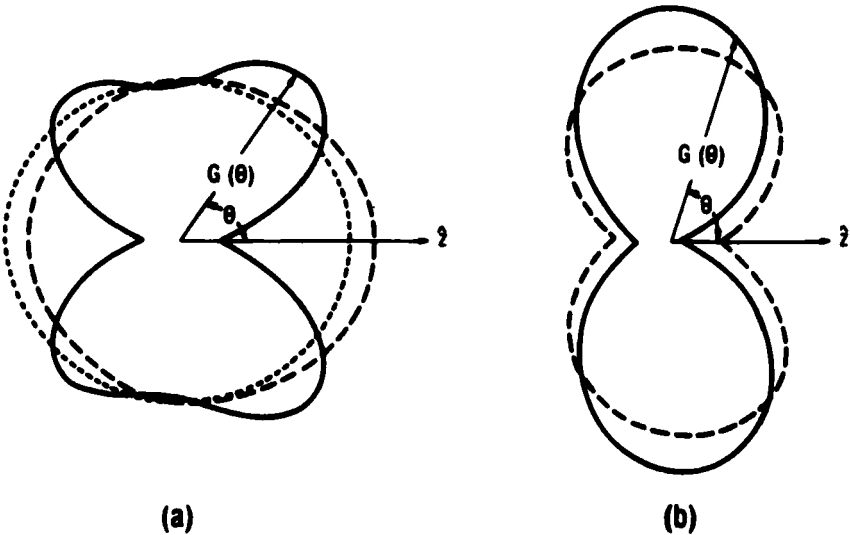


FIGURE 1 Polar plot of the distribution function, $G(\theta)$, as a function of the polar angle, θ . The length of the vector from the origin to the curve shows the magnitude of the distribution function in that direction. The curves shown are for (a) the isotropic film (dotted curve), the poled film with no stress (dashed curve), the poled film under stress (solid curve, $b/kT = 0.5$), (b) $b/kT = 1.0$ (dashed curve), and $b/kT = 1.5$ (solid curve). $E_p = 0.20\text{ MV}/\text{cm}$ in all poled samples.

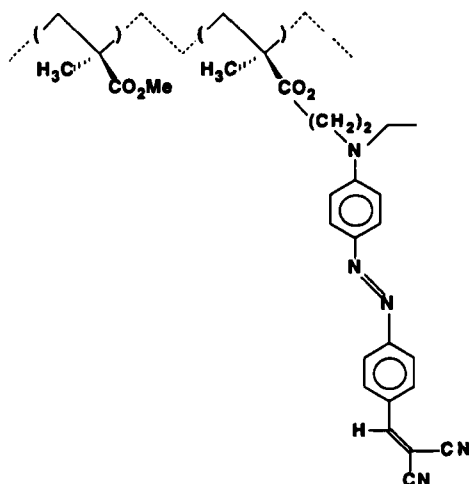


FIGURE 2 Side-chain dicyanovinyl azo methacrylate random copolymer.

nonlinear optical parametric devices are quite different. Electro-optic devices, in addition to requiring a large electro-optic coefficient, also require a low dielectric constant and dielectric loss so that high speed devices can be attained. On the other hand, since only one optical wave is present, the material need only be transparent at this wavelength. This allows near infrared devices to be made from guest molecules which are not transparent in the visible region, and thus possess larger molecular susceptibilities at the operating wavelength. For instance, the polymer in Figure 2 and Table II has an electro-optic coefficient of 18 pm/V at 799 nm . Thus, one can attain useful electro-optic coefficients using high susceptibility guest molecules.

One of the major advantages of using poled-polymer materials in electro-optic devices is the capability of integration with electronic elements on common substrates. With this in mind, silicon wafers are both convenient and attractive foundations on which to fabricate waveguides and build demonstration devices. Optical waveguides are easily formed with polymers by spin coating the material onto a large area wafer. A layer of oxide or glass between the polymer and silicon acts as the cladding material to prevent radiation leakage of the optical mode. By forming thick films capable of supporting several modes, the refractive index may be determined using prism coupling techniques. This standard procedure has been applied to several polymer systems at a variety of optical wavelengths to produce dispersion data such as that shown in Figure 3. While polymethylmethacrylate

TABLE II

Nonlinear optical properties of side-chain dicyanovinyl azo methacrylate polymer film

THICKNESS	REFRACTIVE INDEX	d_{33}	d_{31}	d_{31}/d_{33}
(μm)	$\lambda = 0.8 \mu\text{m}$	(10^{-9} esu)	(10^{-9} esu)	
1.8	1.58	51	17	1/3

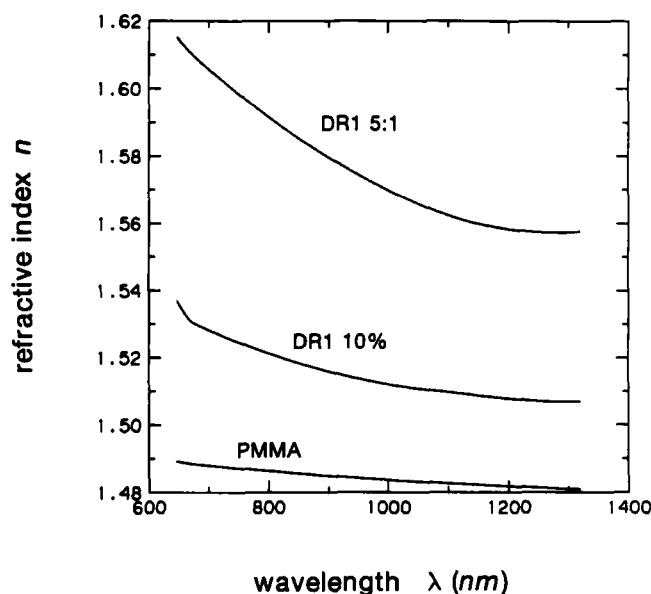


FIGURE 3 Dispersion of guest-host materials. DR1 5:1 is a five to one random copolymer of the Disperse Red 1 azo dye methacrylate and methylmethacrylate. DR1 10% is Disperse Red 1 dye dissolved to 10% by weight in PMMA.

(PMMA) has a refractive index of around 1.48, nonlinear dyes have been incorporated in quantities sufficient to raise the refractive index to the range of 1.5 to 1.6. Due to the strong visible absorption associated with the chromophore, the refractive index is larger for higher energies, showing a dispersion of around 0.04 between wavelengths of 0.6 and 1 μm . Using guest-host polymers of this type, single mode waveguides are formed on glass with films in the 1–2 μm thickness range. Loss measurements using prism coupling have shown that the attenuation is dominated by the properties of the host polymer, usually less than 1 dB/cm . With the technique of corona poling, the polymer film may be aligned using the silicon wafer as the ground plane, thus avoiding the requirement of a top electrode. This permits the further optical characterization of poled materials to determine the birefringence resulting from the poling process.

Figure 4 provides an illustration of a first generation electro-optic device fabricated using poled polymer waveguides on silicon. A planar waveguide modulator was formed by depositing a metal electrode over a portion of the waveguide. A 4 μm layer of phosphosilicate glass was sufficient for the isolation cladding layer on the bottom, a low index of refraction silicone material was used as the upper cladding layer. The upper cladding isolates the electrode material from the waveguide to prevent loading losses. In most cases, the silicone was applied to a thickness of around 2 μm . Finally, the top electrode was sputtered over an area about 0.5 cm in length. Dense glass prisms were used to couple the light into and out of the device.

In order to characterize the phase modulator, the device was placed in one arm

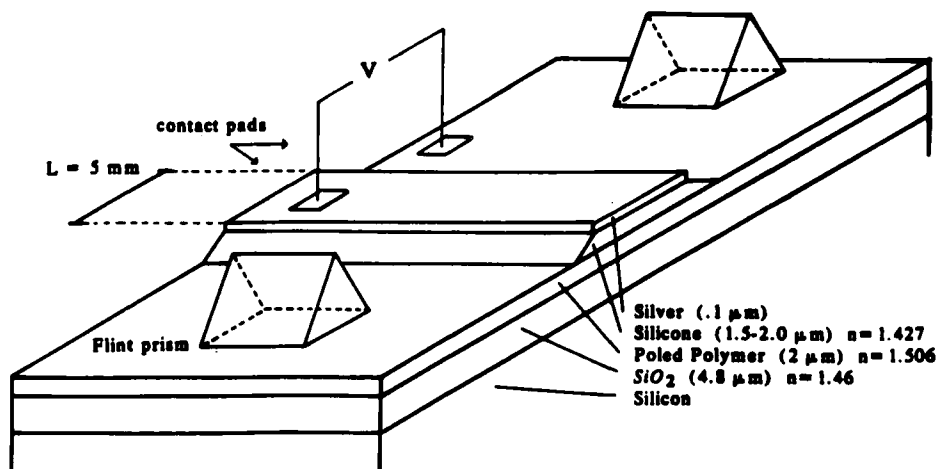


FIGURE 4 Planar waveguide modulator.

of an external Mach-Zehnder interferometer as shown in Figure 5. Light from an infrared laser was divided using a beamsplitter and then passed through the waveguide before being recombined to form a fringe pattern. Voltage applied between the silicon and top electrode was used to modulate the refractive index of the waveguide material. The magnitude of the phase modulation was observed by monitoring the shift in the fringe pattern with either a germanium detector or TV camera. The nonlinear material used in this case was Disperse Red 1 (DR1) dissolved into PMMA at a concentration of around 10%. Previous work has shown that this material when poled at fields around 1 MV/cm results in an electro-optic coefficient of 3 pm/V . With DR1/PMMA as the material, the voltage required to produce a $1/2$ wave of phase retardation is in the range of 80–90 V.

The need for greater light throughput and the capability of making devices such as switches and amplitude modulators requires the fabrication of channel waveguide devices. Figure 6 illustrates the fabrication scheme used for second generation devices. Starting with a similar glass coated silicon wafer, a narrow channel was etched into the glass to a depth less than the glass thickness. The spin-coated

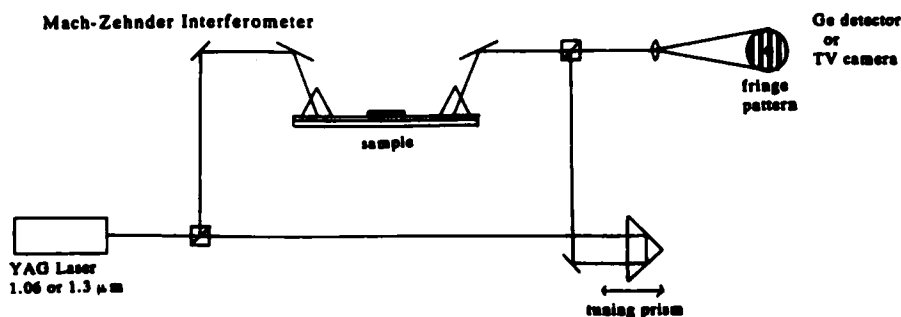


FIGURE 5 External waveguide Mach-Zehnder interferometer.

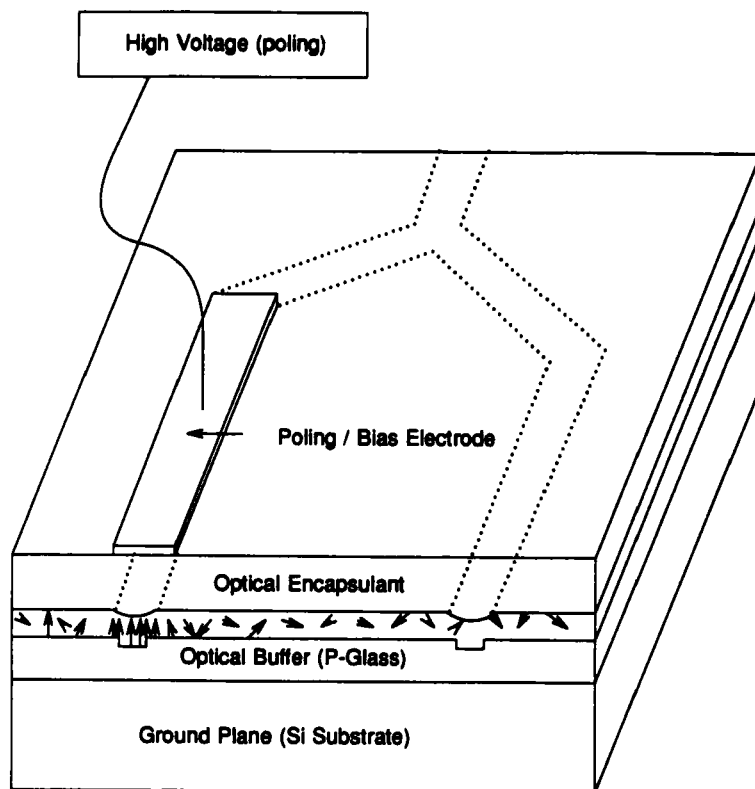


FIGURE 6 Section of Y-branch channel waveguide modulator.

polymer fills into the channel leaving a near planar top surface. Waveguide confinement in the lateral dimension is obtained because the effective mode index of the guided wave is larger in the thicker portion of the channel. Selecting an appropriate channel depth to width ratio assures single mode waveguide operation in the lateral dimension. The waveguide layer was then coated with an encapsulation material on which standard lithography was used to define the top metallization pattern. This procedure has been used to fabricate entire wafers consisting of dozens of straight phase modulators and Y-branch amplitude modulators complete with electrodes, wires, and contact pads. For these devices, it is convenient to use batch processing taking advantage of standard wafer handling equipment. Electric field poling was performed as a last step by applying high voltage to the contact pads during a heating cycle. When the straight phase modulators are measured in one arm of an external interferometer, a determination of the electro-optic coefficient is rapid, accurate, and straightforward. The poling process was confirmed by using TM and TE modes to measure the ratio of the two components of the electro-optic coefficient, $r_{33}/r_{13} = 3$. The straight waveguide was also used as a polarization modulator by placing the waveguide between crossed polarizers. This was useful for insuring that the principal axes of the poled material coincide with the waveguide

axes. Figure 6 shows half of the Y-branch amplitude modulator. For guides of the proper design for single mode operation, efficient extinction was obtained using two electrodes for modulation and tuning of the device. With the polymer shown in Figure 2, a higher refractive index results in thinner device thicknesses and this material is capable of switching voltages in the range of 4–5 V using 1 cm long electrodes. It is clear that as further improvements are made in both the nonlinear materials and processing methods, electro-optical devices capable of high performance will undoubtedly be easily made.

Optical parametric devices, such as second-harmonic generators, parametric oscillators, and parametric amplifiers, require large nonlinear optical coefficients, transparency at all the wavelengths involved, and appropriate phase-matching conditions. Several schemes exist for phase-matching: birefringence phase-matching, guided-mode phase matching, periodic poling phase-matching, and Cherenkov phase-matching.^{11,12} In guided-mode phase matching, the mode dispersion of TM and TE modes of different order are employed to cancel the wavelength dispersion of the material. In this case, however, the energy overlap between these modes is small. Some multilayer structures have been suggested which may get around this requirement. This method may be promising, but intermode scattering may limit efficiency, and an output corresponding to a non-zero order mode may not be focussed to the diffraction limit which may be a problem in some applications, such as optical data storage. Cherenkov phase matching is noncritical, and can be efficient with large susceptibilities, but, again, the output may not be focussed to the diffraction limit.

In order to analyze the possibility of birefringence phase-matching in poled guest-host material the birefringence and dispersion must be determined. Figures 3 and 7 show the measured dispersion and birefringence of our poled guest-host materials. These figures indicate that phase-matching may be possible at certain wavelengths, but as with any scheme for waveguided birefringence phase-matching, a critical fabrication constraint on the thickness is present.

Another possible method of phase-matching is unique to guest-host materials, and requires a critical concentration constraint. The possibility of obtaining phase-matched frequency multiplication by employing anomalous dispersion associated with a strong absorption allowing one component of a mixture to cancel the normal dispersion of another component was proposed over 25 years ago.¹³ Anomalous-dispersion phase-matching is desirable in that the phase-matching is independent of the propagation characteristics of the optical beams; thus, reductions in efficiency due to orientation, beam overlap, spatial dispersion, and beam walk-off are reduced. Furthermore, any tensor coefficient in such a material could be phase-matched with the fields polarized along principle dielectric axes. These factors would allow for high conversion efficiencies without critical beam propagation constraints.

We have demonstrated anomalous-dispersion phase-matched second harmonic generation for the first time using electric field induced second harmonic generation (EFISH) in a liquid solution of propanedinitrile, [2-[[4-(dihexylamino)-2-methylphenyl]methylene]benzo[b]thien-3(2H)ylidene], S,S-dioxide (9CI) known as Foron

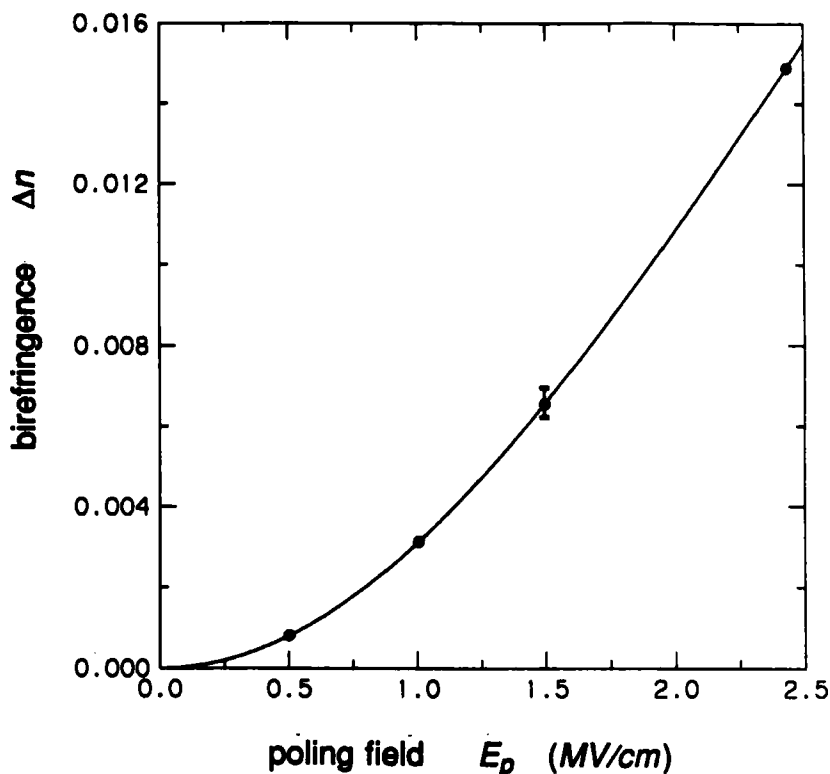


FIGURE 7 Birefringence of DR1 10% by mass in PMMA as a function of poling field intensity.

Brilliant Blue S-R (FBB).¹⁴ This dye has a sharp absorption maximum near 620 nm and a deep absorption minimum near 450 nm.

Anomalous-dispersion phase-matched second harmonic generation at 0.954 μm was accomplished in an electric-field-aligned acetonitrile solution in which the concentration of FBB was varied. Acetonitrile was chosen because it is relatively nondispersive, transparent in the visible, is a good solvent, is nonhydroxylic, and is noncorrosive toward the cell's electrodes. The EFISH experiment was performed in acetonitrile as a function of concentration of Foron Brilliant Blue S-R at a fundamental wavelength of 0.954 μm . The dispersion ($n_{2\omega} - n_{\omega}$) for measurements at various concentrations was determined from the coherence length, and is plotted in Figure 8. The intercept for zero dispersion was determined from this plot to be at approximately 0.044 M, and the molar dispersivity was found to be 0.2313 M^{-1} . A 0.1 M solution was prepared and EFISH measured on dilution of this stock. The concentration dependence is shown in Figure 9. The peaked behavior indicating a factor of 50 enhancement at approximately 0.045 M is consistent with the extrapolation in Figure 8, and clearly signifies phase-matched second harmonic generation.

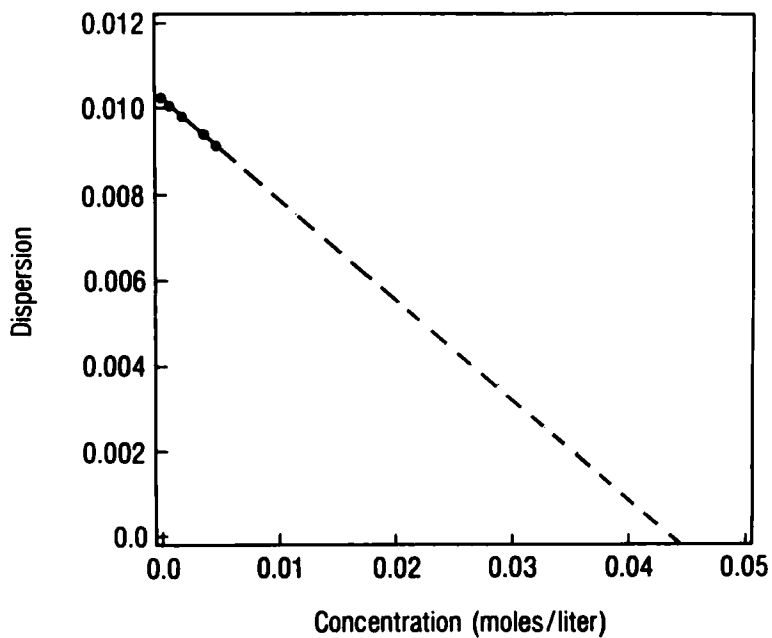


FIGURE 8 Dispersion versus concentration for solutions for Foron Brilliant Blue S-R in acetonitrile.

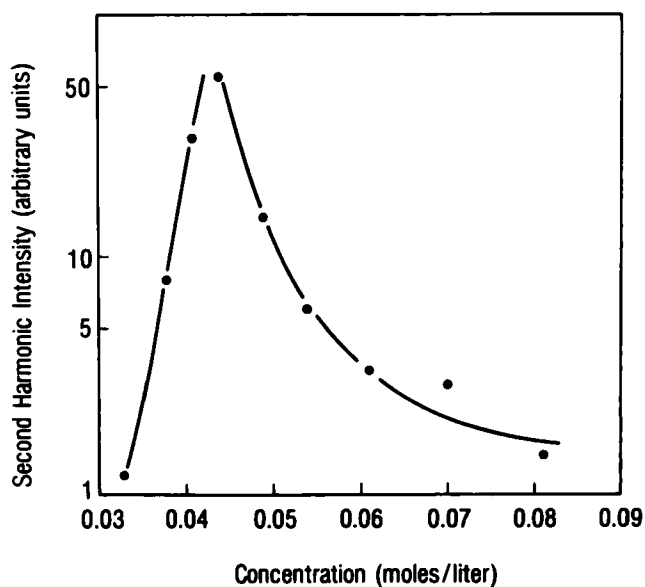


FIGURE 9 Second harmonic intensity versus concentration for solutions of Foron Brilliant Blue S-R in acetonitrile near the anomalous-dispersion phase-matched condition.

In conclusion, the material and fabrication flexibility of poled polymer glasses have quickly led to a variety of demonstration electro-optic devices. It is also hoped that this flexibility will also help to generate efficient nonlinear optical devices. Meanwhile, work on material improvements and control of device fabrication processes continues. Both trends point to an expanding technology in poled polymer glasses for second-order nonlinear optical devices and systems.

Acknowledgments

The authors gratefully acknowledge the contributions of D. L. Fish, H. M. Gordon, L. A. King, J. L. Markham, and H. E. Zahn. A portion of this work was performed at Sandia National Laboratories supported by the U.S. Department of Energy under contract number DE-AC04-76DP00789.

References

1. D. S. Chemla and J. Zyss, ed., *Nonlinear Optical Properties of Organic Molecules and Crystals* (Academic Press, New York, 1987).
2. A. J. Heeger, J. Orenstein and D. R. Ulrich, ed., *Nonlinear Optical Properties of Polymers* (Materials Research Society, Pittsburgh, 1988).
3. K. D. Singer, M. G. Kuzyk and J. E. Sohn, "Second-Order Nonlinear Optical Processes in Orientationally Ordered Materials: Relationship Between Molecular and Macroscopic Properties," *J. Opt. Soc. Am.*, **B4**, 968 (1987).
4. J. D. Le Grange, M. G. Kuzyk and K. D. Singer, "Effects of Order on Nonlinear Optical Processes in Organic Materials," *Mol. Cryst. Liq. Cryst.*, **150b**, 567 (1987).
5. T. Rasing, Y. R. Shen, M. W. Kim, P. Valint and J. Bock, "Orientation of Surfactant Molecules at a Liquid-Air Interface Measured by Optical Second-Harmonic Generation," *Phys. Rev.*, **A31**, 537 (1985).
6. M. G. Kuzyk, K. D. Singer, H. E. Zahn and L. A. King, "Controlling the Second-Order Nonlinear Optical Tensor Properties of Poled Films with Stress," *1988 Technical Digest Series*, **9**, "Nonlinear Optical Properties of Materials" (Optical Society of America, Washington, D.C., 1988).
7. M. G. Kuzyk, K. D. Singer, H. E. Zahn and L. A. King, "Second-Order Nonlinear-Optical Tensor Properties of Poled Films Under Stress," *J. Opt. Soc.*, **B6**, 742 (1989).
8. K. D. Singer, M. G. Kuzyk and J. E. Sohn, "Orientationally Ordered Electro-Optic Materials," in *Nonlinear Optical and Electroactive Polymers*, P. N. Prasad and D. R. Ulrich, eds. (Plenum, New York, 1988).
9. K. D. Singer, M. G. Kuzyk, W. R. Holland, J. E. Sohn, S. J. Lalama, R. B. Comizzoli, H. E. Katz and M. L. Schilling, *Appl. Phys. Lett.*, **53**, 1800 (1988).
10. H. E. Katz, K. D. Singer, J. E. Sohn, C. W. Dirk, L. A. King, and H. M. Gordon, "Greatly Enhanced Second-Order Nonlinear Optical Susceptibilities in Donor and Acceptor Organic Molecules," *J. Am. Chem. Soc.*, **109**, 6561 (1987).
11. G. I. Stegeman and R. H. Stolen, "Waveguides and Fibers for Nonlinear Optics," *J. Opt. Soc. Am.*, **B6**, 652 (1989).
12. K. D. Singer and J. E. Sohn, "Organic Materials for Second-Order Nonlinear Optical Devices," in *Electroresponsive Molecular and Polymeric Systems*, T. Skotheim, ed. (Marcel-Dekker, in press).
13. J. A. Armstrong, N. Bloembergen, J. Ducuing and P. S. Pershan, "Interaction Between Light Waves in a Nonlinear Dielectric," *Phys. Rev.*, **127**, 1918 (1962). See also P. A. Franken and J. F. Ward, "Optical Harmonics and Nonlinear Phenomena," *Rev. Mod. Phys.*, **35**, 23 (1963).
14. P. A. Cahill, K. D. Singer and L. A. King, *Opt. Lett.*, **14**, 1137 (1989).